



Trigg, M. A., Bates, P. D., Wilson, M. D., Schumann, G. J., & Baugh, C. A. (2012). Floodplain channel morphology and networks of the middle Amazon River. *Water Resources Research*, 48(10), [W10504]. <https://doi.org/10.1029/2012WR011888>

Publisher's PDF, also known as Version of record

Link to published version (if available):
[10.1029/2012WR011888](https://doi.org/10.1029/2012WR011888)

[Link to publication record in Explore Bristol Research](#)
PDF-document

An edited version of this paper was published by AGU. Copyright 2012 American Geophysical Union.

University of Bristol - Explore Bristol Research

General rights

This document is made available in accordance with publisher policies. Please cite only the published version using the reference above. Full terms of use are available:
<http://www.bristol.ac.uk/red/research-policy/pure/user-guides/ebr-terms/>

Floodplain channel morphology and networks of the middle Amazon River

Mark A. Trigg,¹ Paul D. Bates,¹ Matthew D. Wilson,² Guy Schumann,¹ and Calum Baugh¹

Received 19 January 2012; revised 28 June 2012; accepted 16 August 2012; published 6 October 2012.

[1] Floodplain channels are important components of river-floodplain systems and are known to play a key role in hydrodynamic exchange and sediment transport. The Amazon floodplain exhibits complex networks of these channels, and despite their potential importance to this globally important wetland system, these floodplain channels are relatively unstudied. The research presented here is the first systematic and detailed study of the network and morphologic characteristics of a large number of these channels in the middle reach of the central Amazon River using analysis of data derived from Landsat Enhanced Thematic Mapper Plus (ETM+) mosaic and field survey. Our findings show that the channels are ubiquitous, their width varies widely, and some of their characteristics can be fitted using power laws, potentially much like the self-similar or fractal-like behavior hypothesized for other types of fluvial networks. In all, 96% of the floodplain channels are not wide enough to be represented well, or at all, in the ~90 m Shuttle Radar Topography Mission data. Channel depths are tied closely to the local amplitude of the passing main river flood wave (p value of 0.75), except where there are local runoff inputs, which results in substantially deeper channels which provide preferential flow paths across the floodplain. Channel networks imply that areas of the floodplain function for large parts of the flood cycle as separate hydrogeomorphic land units, here termed floodplain hydrological units (FHUs). These hypothesized FHUs also have distinct spatial and pattern characteristics, and it is suggested here that their differences could provide the beginnings of a framework for understanding the detailed hydrodynamics of the floodplain. In particular, different types of FHUs have differences in flood water source, which will have important implications for biogeochemical studies of the wetlands.

Citation: Trigg, M. A., P. D. Bates, M. D. Wilson, G. Schumann, and C. Baugh (2012), Floodplain channel morphology and networks of the middle Amazon River, *Water Resour. Res.*, 48, W10504, doi:10.1029/2012WR011888.

1. Introduction

[2] The Amazon River basin is a large, globally important, biosphere with a strong interdependence with regional and global climates. At the core of the Amazon biosphere is the river and its floodplain and it is estimated that 20% of the Amazon lowland basin is covered by permanently or seasonally flooded wetlands [Junk, 1993]. Interfluvial swamps and flooded savannas cover extensive areas in some regions, but it is the river floodplains which are the dominant wetland habitat in the Amazon [Forsberg *et al.*, 2000]. Wetland mapping of the central part of the Amazonia lowland, an area of some 1.7 million km², shows that the total wetland area accounts for 17% of this area, around ~300,000 km². In addition, nearly 70% of this wetland area is forested and

51% is composed of the floodplains of the main river stem and its tributaries [Hess *et al.*, 2003].

[3] The flow in the Amazon system shows an annual monomodal flood cycle closely correlated with the main rainfall season. The size and regularity of this monomodal flood wave has profound implications for the river and its floodplain, with the dynamic exchange of water between the channel and floodplain playing a central role in biological and biogeochemical processes in the Amazon basin [Junk and Piedade, 1993; Melack and Forsberg, 2001; Wittmann *et al.*, 2004]. Transfer of floodwater from the main channel onto the floodplain and the subsequent draining of the floodplain occurs through a combination of over-bank diffusive flow and channelized flows through numerous floodplain channels [Mertes *et al.*, 1995, 1996]. From hydrological modeling, Richey *et al.* [1989] states that as much as 30% of the peak flow in the main river channel is derived from water that has passed through the Amazon floodplain. In particular, the floodplain channels siphon off sediment laden river water into the floodplain and subsequently return it when main stem water elevations are below bankfull, thus complicating the dynamics of floodplain wetting and drying. In addition, water also enters the floodplain from terra firma runoff, and tracking of this input and its

¹School of Geographical Sciences, University of Bristol, Bristol, UK.

²Geography, Faculty of Science and Agriculture, University of the West Indies, St. Augustine, Trinidad and Tobago.

Corresponding author: M. A. Trigg, School of Geographical Sciences, University of Bristol, Bristol BS8 1RJ, UK. (mark.trigg@bristol.ac.uk)

mixing with river-derived floodwaters led *Mertes* [1997] to identify a meteoric-water-dominated “perirheic zone” on the inundated floodplain. In effect, *Mertes* [1997] was the first to identify that restricted mixing of waters derived from different sources may lead to a distinct zonation of the floodplain. Further, *Mertes* [1997] showed that the local variations in flow volume, flow dynamics, sediment load, nutrient content and ecology that result from this zonation could have implications for a variety of floodplain processes. Hence *Mertes* [1997] was the first to suggest that the Amazon floodplain is composed of at least two distinct functional units based on water source: river dominated and local meteoric water dominated.

[4] Lakes cover a large proportion of the Amazon floodplain and are important ecosystems that have received significant attention in the field of limnology [e.g., *Lesack*, 1995; *Stolum*, 1998; *Engle and Melack*, 2000; *Bonnet et al.*, 2005; *Barroux et al.*, 2006; *Bonnet et al.*, 2008]. Lake studies show that floodplain channels provide important inputs to and outputs from the floodplain lake systems even during low to mid water conditions, and can experience reversal in flow direction depending upon hydraulic conditions [*Lesack and Melack*, 1995]. While a few floodplain channels connected to particular lake sites have been studied, the characteristics and behavior of the reach-scale floodplain channel system has received comparatively little detailed research attention despite mapping and sedimentation studies showing that the floodplain channels are an important part of the Amazon riverine landscape [*Mertes et al.*, 1995, 1996].

[5] Floodplain channels provide important routes for conveying sediment from the main river into the floodplain [*Mertes et al.*, 1993] and the quantity and characteristics of the channels vary along the length of the Amazon main stem [*Mertes et al.*, 1996; *Toivonen et al.*, 2007]. *Mertes et al.* [1996] identified that (1) there were larger floodplain channels (800–2000 m width) present in the downstream main river reaches, (2) smaller floodplain channels (<100 m wide) were also present in all reaches, and (3) navigation chart depths for floodplain channels (where available) showed no correlation with downstream main river distance. *Alsdorf* [2003] identified floodplain channel flow path distance (along the channels) from the main river for locations in the Amazon floodplain and showed that water level changes measured with space shuttle based interferometric synthetic aperture radar (SAR) data were inversely correlated to this distance. This work highlights the convoluted nature of the flow paths on the floodplain and the effect on floodplain water levels caused by the balance between water supply and drainage, as well as water storage. *Alsdorf et al.* [2005] attempted to model this complex floodplain flow through a simple diffusion model of the floodplain with the aim of moving away from the commonly used assumption that floodplain water levels equate to channel water levels. While the *Alsdorf et al.* [2005] model shows some broad correlation with interferometrically measured water level changes, more recent work [*Alsdorf et al.*, 2007] shows the water level changes across the floodplain are more complex than thought previously and that some of these changes can be spatially correlated with the floodplain channels.

[6] Two particularly relevant studies of floodplain channels on river systems other than that of the Amazon are those of *Day et al.* [2008] and *Rowland et al.* [2009].

Day et al. [2008] studied tie channels (connecting the main river to floodplain lakes) and small tributary channels on the floodplain of the Fly River in Papua New Guinea, a river similar to the Amazon in that it has a low-gradient, wet, and wide floodplain with relatively low sediment load. *Day et al.* [2008] describe a deposition web formed by these floodplain channels conveying river sediment deep into the floodplain. *Rowland et al.* [2009] look at the formation and maintenance of these tie channels in more detail on three separate river systems and highlight the flow reversals that occur in these channels as key to the maintaining their morphology.

[7] This above review of previous work on floodplain channels and floodplain water level dynamics suggests that a study of the reach-scale behavior and connectivity of the floodplain channel system would be an important step toward understanding the reasons for the observed complex spatial heterogeneity, although to date this has not been possible due to a lack of sufficiently spatially detailed data. However, newly available sources, such as elevation data from the Shuttle Radar Topography Mission (SRTM) and other remote sensing data sets, are transforming the study of the Amazon and providing new opportunities to study the dynamics of the flood wave, either directly [*Alsdorf et al.*, 2005; *Martinez and Le Toan*, 2007] or through incorporation into hydraulic models to simulate the hydrodynamics [*Wilson et al.*, 2007]. *Wilson et al.* [2007] postulated that accurate simulation of the hydrodynamics on the floodplain was hampered by an inability of the SRTM terrain data to resolve small scale topographic features that control floodplain drainage and by the omission of floodplain hydrologic processes from the model that they used. Given the observed scale and quantity of the floodplain channels, it is very likely that they play an important role in the hydrodynamics of the floodplain processes. How well these channels are represented in the available digital elevation data appears to be crucial to the accurate simulation of river and floodplain hydrodynamics [*Wilson et al.*, 2007].

[8] In this paper, we present the first systematic study of the floodplain channels and their characteristics for a 285 km middle reach of the Amazon floodplain using spatial analysis of remote sensing data and field survey. Specifically, the paper has three aims: (1) to undertake a reach-scale mapping of the entire floodplain channel network visible in remote sensing imagery to determine spatial patterns and network connectivity, (2) to undertake a large scale field based survey of floodplain channels (>1000 line km) to determine width versus depth relationships and examine how these may be influenced by local hydrology and base river levels, and (3) based on the above analysis, to determine whether floodplain channels can be classified into different functional types.

[9] The overall aim of the paper is therefore to explore whether a more detailed understanding of the floodplain channel system can aid in understanding the complex heterogeneity and functioning of the Amazon floodplain and thereby improve attempts to simulate river and floodplain hydrodynamics.

2. Methodology

2.1. Study Area and Context

[10] The study area is centered on the Solimões and Purus confluence upstream of Manaus (Figure 1) and

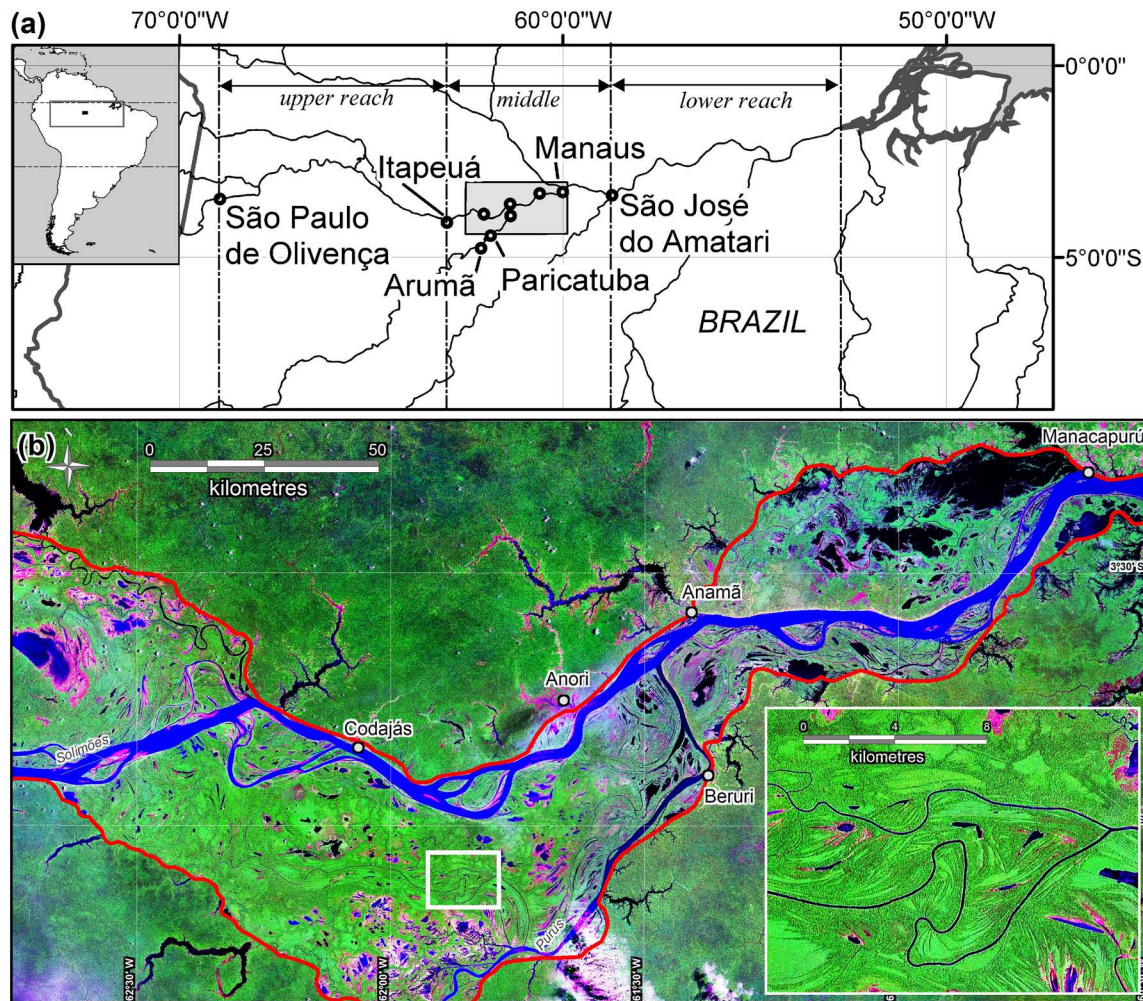


Figure 1. Study area. (a) Location overview, showing the study area centered on the Solimões River and Purus River confluence and reach divisions after *Mertes et al.* [1996]. (b) Tri-Decadal Global Landsat Orthorectified Pan-Sharpened ETM+ Mosaic (1999–2003), courtesy of the U.S. Geological Survey and downloaded from their Global Visualization Viewer (GLOVIS), with inset box in white. The floodplain boundary is shown as a thick red line [*Hess et al.*, 2003]. Circles indicate population centers.

covers an area of 30,000 km², a significant portion (~50%) of the middle reach of the three main stem floodplain reaches defined by *Mertes et al.* [1996] and *Dunne et al.* [1998] (also shown on Figure 1). Each of the main stem reaches is defined by distinct geomorphology linked to river slope, sediment transport and geological controls: (1) the upper reach (São Paulo de Olivença to Itapeuá), dominated by floodplain deposition through channels, producing intricate scroll bar topography with hundreds of long, narrow lakes, (2) the middle reach (Itapeuá to São José do Amatari), which is relatively narrow with some lakes and little evidence of channel migration, and (3) the lower reach (downstream of São José do Amatari) characterized by channels restricted by levee building and overbank deposition, resulting in a flat floodplain with a patchwork of large, irregular, shallow lakes.

[11] A 285 km reach of the Solimões (Amazon River) passes from west to east through the study area and a 107 km reach of the Purus tributary flows from the south to join it in the center. The Solimões River is around 3–5 km

wide at this location and the floodplain varies from 30 to 50 km across. It was not possible to carry out this study on the entire central Amazon floodplain due to issues of scale and field measurement logistics. We chose our study site in the middle reach and we consider in the discussion below how broadly representative this middle reach may be of the entire floodplain, while acknowledging that it is still a subset of the floodplain as a whole.

[12] Both *Mertes et al.* [1996] and *Latrubesse and Franzielli* [2002] describe geomorphological features in the middle reach that are also present in both upstream and downstream reaches; namely, scroll bar topography with long, narrow lakes, river levees with overbank deposits and large, irregular, shallow lakes. *Mertes et al.* [1995] determined using remote sensing of hydrology and vegetation that the middle reach had the most diversity of wetland classes and posited that this was due to exposure to a wider variety of water types and landforms present in this location.

[13] The Amazon floodplain is a complex mosaic of lakes, floodplain channels, scroll bars and overbank deposits,

where local patterns are controlled by the large scale structure of the Amazon craton [Mertes *et al.*, 1996]. This continental scale lithospheric feature is interrupted by tectonic arches that bound intracratonic basins which are slowly infilling with sediment [Dunne *et al.*, 1998]. Potentially of particular importance here is the Purus arch which crosses the 285 km reach studied in this paper on an approximate north-south alignment. Mertes *et al.* [1996] hypothesized that because of this tectonic feature the valley narrows, the water surface gradient decreases, sediment is deposited, and there is a regionally low exchange of water and sediment between the main stem and floodplain channels.

[14] The middle reach of the central floodplain identified by Mertes *et al.* [1996] has been shown by Latrubesse and Franzinelli [2002] to consist of a complex system of Quaternary sedimentary units of different ages, with the present position of the channel as well as the morphology and size of the alluvial plain related to neotectonic linear features. These neotectonic features constrain the channel to a series of straight sections with a relatively small number of islands and anabranches. In contrast to Mertes *et al.* [1996] and Dunne *et al.* [1998], Latrubesse and Franzinelli [2002] do not highlight the Purus arch explicitly as an important feature in the current geomorphology of the river and floodplain in this central reach. However, Latrubesse and Franzinelli, [2002] do state that the alluvial plain is broadest where the river crosses faulted sunken tectonic blocks, and presumably these are bounded by the tectonic arches as stated by Dunne *et al.* [1998]. There is considerable uncertainty over the exact location and extent of these tectonic arches given that information on them is scarce and restricted to unpublished oil exploration documents [Dunne *et al.*, 1998], which limits the inference of their effects to generalizations. Rossetti *et al.* [2005] emphasize

that most of the tectonic arches are Paleozoic or Mesozoic structures buried under a mantle of Cretaceous and Cenozoic deposits, and uses the Purus Arch as an example of what has previously been considered to be an important vicariance feature, but is actually a geologic structure that occurs under more than 1000 m of Cretaceous rocks of the Alter do Chão Formation. It could be inferred from this that the Purus arch may not provide a strong or direct control on the fluvial hydraulics in this middle reach, and that more recent neotectonic features may have a more significant role to play in terms of the detailed hydrodynamics of the floodplain. Given the uncertainty surrounding the actual location of the Purus Arch and its relative importance on river hydraulics, there is clearly a need for further research in this area.

[15] A plot (Figure 2) of floodplain width for all three reaches from a floodplain boundary derived from the more recent work by Hess *et al.* [2003] shows a much greater variation in floodplain width along river than presented by Mertes *et al.* [1996] from data available at that time. Hess *et al.* [2003] used 100 m resolution synthetic aperture radar imagery from the Japanese Earth Resources Satellite-1 to map wetland extent in the central Amazon region. We used automated polygon width extraction in ArcGIS to measure the floodplain width of the central Amazon River floodplain extent polygon derived from the mapping by Hess *et al.* [2003] and shown in Figure 4b of their paper. Widths were measured perpendicular to the floodplain centerline at 5 km intervals and this is plotted against river distance downstream of Iquitos. The location of the study area is also shown in Figure 2 and it can be seen from this that the study area is in one of the wider sections of the central floodplain just upstream of one of the narrowest sections and, in terms of floodplain width at least, could be considered representative of the whole floodplain. This more detailed variation in

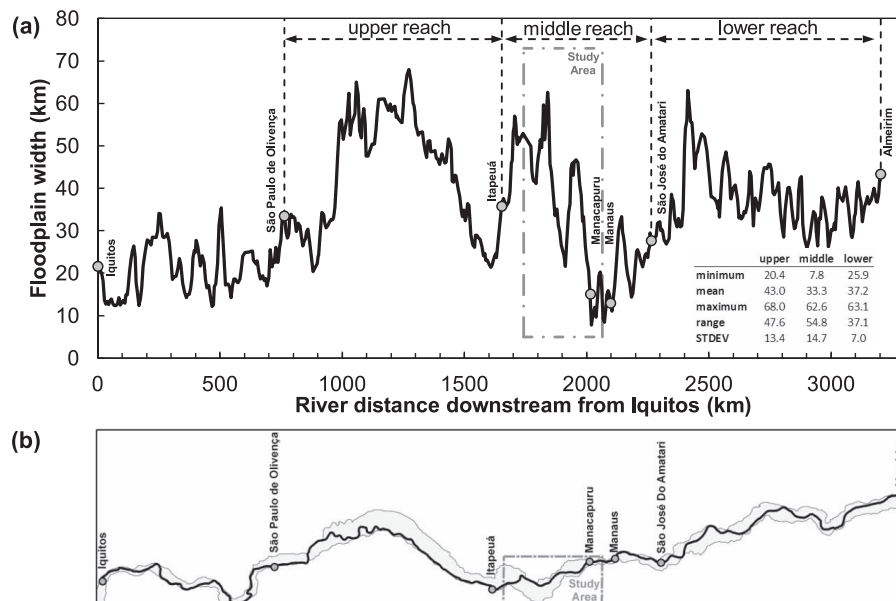


Figure 2. (a) Plot of floodplain width by along-river distance, downstream of Iquitos, derived from Hess *et al.* [2003]. Three main reach divisions are delineated [Mertes *et al.*, 1996], with width statistics by reach in the table in the bottom right. Study area is also highlighted by the centerline dot-dashed gray box. Towns are shown as labeled circles. (b) Plot of river centerline (black) and floodplain extent (gray boundary), with location of study area.

floodplain width than previously demonstrated may mean that the central reach has more transitional characteristics than previously supposed and that this reach is therefore a reasonable location in which to carry out our study.

[16] Previous work in this our study reach by *Latrubesse and Franzinelli* [2002] used sediment surveys, radiocarbon analysis, Landsat images and JERS-1 images to undertake geomorphologic and sedimentologic mapping of fluvial deposits. From this mapping *Latrubesse and Franzinelli* [2002] recognize three floodplain units for the middle reach of the central Amazon: (1) older scroll-dominated plain, (2) an impeded floodplain, and (3) a channel-dominated floodplain. The older scroll-dominated plain is a lower terrace in which scroll morphology is well developed, indicating a meandering Amazon or dynamic secondary channel (paranas). The impeded floodplain is characterized by a number of round or irregularly shaped lakes on a very flat surface. Some of the lakes are connected to the main stem by channels while others are not, and the units are not totally flooded every year. The channel-dominated floodplain is a complex mosaic of fluvial forms: mainly channels, active sandbars, levees, scroll-dominated plain, islands and abandoned channel systems. By the definition of *Mertes* [1997], the impeded floodplain (unit 2 above) is *Mertes'* meteoric-water-dominated “perirheic zone” and the channel dominated floodplain (unit 3) is the river-dominated floodplain. The older scroll-dominated plain (unit 1) seems to be more complex in terms of water source than the other two units as it contains secondary paranas channels which are connected to the main river and to small tributaries providing local runoff input.

2.2. Landsat Mosaic Analysis

[17] Landsat 7 data were used to quantify image measurable floodplain channel parameters: length, width and connectivity. Specifically, the Tri-Decadal Global Landsat Orthorectified Pan-Sharpener ETM+ Mosaic (1999–2003) with a spatial resolution of 15 m was used, courtesy of the U.S. Geological Survey and downloaded from their Global Visualization Viewer (GLOVIS). This spatial resolution is sufficient to resolve most of the floodplain channels that are observable from above, with smaller channels likely to be obscured from overhead by overhanging vegetation. Landsat TM images have already had their utility demonstrated in the study of the Amazon wetlands [*Mertes et al.*, 1993, 1995; *Peixoto et al.*, 2009]. Their free availability, well documented characteristics, long-running program (since 1972) together with their wide spatial coverage and high resolution make them suitable for studying the floodplain channels. Where available, Google Earth Geocye 1.65 m multispectral resolution images, detailed enough to resolve individual tree canopies of 1–2 m across, were used for comparison and to aid with the interpretation of features in the Landsat mosaic.

[18] The primary methodology involved manual digitization of all visible floodplain channels in the 30,000 km² study area using GIS software to produce a vectorized data set of channels derived using a consistent methodology. Although there has been some success in applying automated and semiautomated methods of stream network extraction to remote sensing images [e.g., *Dillabaugh et al.*, 2002; *Pavelsky and Smith*, 2008], many of these methods use assumptions related to the flow behavior of typical rivers that may

not be applicable to the complexity of the Amazon floodplain channel network. *Als Dorf* [2003] notes this complexity problem when applying automated network extraction methods to SAR analog topographic data in the Amazon floodplain. Once a better understanding of the characteristics of the floodplain channels is obtained, it may be appropriate to apply more automated methods.

[19] Channels digitized included all visible channels except for the main Solimões channel and Purus tributary channel, and include minor tributaries feeding the floodplain from small local runoff catchments. Channels draining water out of the study area and therefore not directly contributing to the river and floodplain within the domain were excluded from the analysis. Figure 1b shows the Landsat Enhanced Thematic Mapper Plus (ETM+) mosaic for the study area together with a close-up inset box. Water bodies are very clear on the false color image composites as black or dark blue objects with pink areas indicating exposed beds at low water. This contrasted sharply with the green vegetation covering much of the images. Channels were digitized in reaches, with a separate reach defined where there was an obvious branch or connection, analogous to river order in a river drainage system.

[20] The Landsat ETM+ mosaics are composed of cloud free images over several years, so cannot be taken as a snapshot in the flood wave cycle. Most of the images used appear to come from the flood recession and low-water period when there is generally less cloud cover. This means that in the mosaic image, the floodplain is well drained revealing large areas of lake bed or sediment deposits. The smaller channels of 20–30 m width, were the most difficult to digitize, as this was close to the image spatial resolution, making them less clear. In addition, overhanging tree canopies obscure a greater proportion of the width of the smaller channels. Floating macrophytes blocking channels also obscured sections of channels in the images and where available (~80% of study area), the Google Geocye images were helpful in determining continuity with more confidence. Canopy and macrophyte obscured channels would present severe continuity challenges for automated methods.

[21] For each of the vectorized channel reaches, a number of different physical characteristics were quantified and assigned to an attribute table. The width of each channel was taken as the mean of three distance measurements from the Landsat mosaic, one at both ends and one in the center of the reach. Where a channel passes through a lake, the width of channelized section was used rather than the lake width. Channel widths were rounded to the nearest 10 m due to the image resolution and the smallest channels detectable clearly are around 20 m wide. Length was extracted automatically from the GIS object and rounded to the nearest meter.

[22] Another important characteristic of the floodplain channels is their source of water *Mertes* [1997]. *Mertes* [1997] identifies inundation of floodplains by regional water, that is, overbank flow from the main river channel, and local water, that is, groundwater, hyporheic water, local tributary water, and direct precipitation onto the floodplain. Of these sources, we can identify by channel connection, main river and local tributary water. Other than the Purus River in the study area, most of the tributaries are very localized and small, so we refer to them here as “local

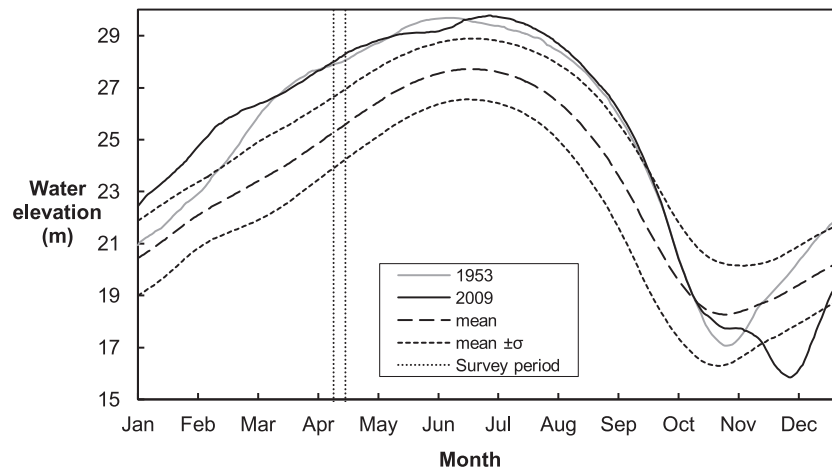


Figure 3. Manaus mean water elevation curve with $\pm\sigma$, together with 2009 and 1953 data. Field survey period is highlighted.

runoff” to avoid confusion with the main Amazon tributaries. There are two main sources of water on the floodplain (other than direct rainfall): river floodwater and local runoff from the small river terrace catchments lining the floodplain (essentially very small tributaries). Digitized channels located outside the floodplain boundary derived from Hess *et al.* [2003] are local river terrace runoff channels draining their own small catchments and some of these include ria lakes in drowned valleys. These channels were classified as having local runoff input. Digitized channels within the floodplain boundary that were not connected to catchments external to the floodplain boundary were classified as having no local runoff. A few of the larger floodplain channels had a clear connection to the main river channel at both the upstream and downstream ends (for example, around river islands) and could be considered small side branches of the main river, so these were classified as main river channel. Finally, channel reaches that are connected to each other were assigned to a common network group.

2.3. Bathymetric Survey

[23] A limitation of the remote sensing data that are available for the Amazon is the difficulty the instruments have in penetrating the water surface, resulting in a knowledge gap regarding bathymetry of the water bodies of the Amazon. For the main river, a significant amount of original main channel bathymetric data was collected in 2005 for reaches of the Amazon and Purus Rivers by Wilson *et al.* [2007]. These data were utilized in full for the research on the hydraulics of the main channel flood wave carried out by Trigg *et al.* [2009].

[24] For the floodplain itself, very few bathymetric data are available, except for spot depths from dated navigation charts [Mertes *et al.*, 1996; Latrubesse and Franzinelli, 2002]. Some location specific bathymetric data have been collected for lake studies [Panosso *et al.*, 1995; Bonnet *et al.*, 2005], but it is difficult to apply these findings more broadly to the wider floodplain. Bonnet *et al.* [2008] combined field measured water elevations with flood extents derived from JERS-1 images to derive a low- to high-water bathymetric DEM of the Curuaí floodplain near Óbidos. However, for permanently flooded lake areas and nine

small floodplain channels connecting the lakes to the main river, spot measurements of depth from the field were still required to estimate bathymetry. Barbosa *et al.* [2006] carried out a bathymetric survey of the Curuaí floodplain lakes using a sonar GPS unit and found that these data could be used together with Landsat images to estimate the floodplain water storage volumes.

[25] To address the lack of bathymetric data for the floodplain channels, a dedicated survey of the channels within the study area was undertaken as part of the research presented in this paper. The overall aim of the field survey was to survey the depth and width characteristics of the floodplain channels, ground truthing the characterization of floodplain channel types and widths identified in the Landsat mosaic analysis. Given the rarity of this type of data, the sonar data collected has been made available as auxiliary material to this paper.¹

[26] The survey was carried out for a total of 9 days between 7 and 15 April 2009. The high-water period for the study area is between April and September, with the flood peak usually occurring at the end of June or beginning of July. The year 2009 turned out to be an unusual year, with the peak water level in Manaus reaching 29.75 m (local datum), breaking the previous 106 year record set in 1953 of 29.69 m. This meant that at the time of the survey, water levels were already at the mean annual maximum level of 27.72 m for Manaus, see Figure 3. The implication is that the survey was carried out at a stage in the flood cycle that is equivalent to the mean annual high-water period, thus measured depths are likely to be in the range of the maximum observable. It also means that the variations of water levels across the floodplain are likely to be at a minimum as evidenced by [Alsdorf *et al.*, 2007].

[27] A 6 m long aluminum hulled boat was used for the survey with a draft of just under 1 m and a daily range of around 220 km. The small boat allowed access to the narrower floodplain channels and the survey was conducted using the towns of Anamá, Anori, and Codajás along the

¹Auxiliary material data sets are available at <ftp://ftp.agu.org/apend/wr/2012/wr011888>.

main stem as bases. In order to collect bathymetric data, a Garmin 450S combined sonar and GPS System was used with a transom mounted dual frequency sensor (50 and 200 KHz). The unit has a depth range of 457 m (dual frequency) and transmit power of 500 W (RMS). A memory card allowed transfer of the recorded data to a laptop on a daily basis. Most of the time a 2 s recording interval was used, which with an average boat speed of around 30 km h⁻¹ gave a mean sonar point spacing of around 16 m.

[28] Two forms of bathymetric survey were carried out on the floodplain channels. Longitudinal profiles of the channels were taken by traversing along the length of the channels. Where possible the boat was steered down the center of the channels in order to measure the central channel depth, away from the banks. Perpendicular channel cross sections were also surveyed periodically along the channel lengths. Start and end points of the cross sections were as close to the overhanging bank vegetation as was possible. Due to the sheer number of channels in the study area and issues of navigability, it was not possible to survey all the channels. However, an attempt was made to cover as many different types of channel as possible (e.g., island, floodplain, minor tributary), over a range of widths, and across the full study area.

[29] A Longridge Pin Point laser distance rangefinder was used to measure the widths of the channels. This uses a six times optical magnification and has a range of up to 400 m with ranging error of ± 1 m to $\pm 0.1\%$ of the range. Channel widths were measured at varying intervals during the longitudinal channel traverses. The laser range finder was aimed at both banks, one after the other and readings taken from the edge of the vegetation. A waypoint was recorded on the sonar GPS each time a width was measured in order to locate the width measurement spatially.

3. Results and Discussion

3.1. Floodplain Channel Spatial Characteristics

[30] A total of 1762 channel reaches were digitized from the Landsat ETM+ mosaic within the study area (Figure 4). The channels ranged in width from 900 m down to the minimum resolvable width of around 20 m, with a mean width of 47 m. In length the channels varied from 160 m to 67 km, with a mean of 5.3 km and total length of 9293 km. Error is expected to be less than one pixel resolution (15 m) and geolocation accuracy does not affect absolute width or length measurements.

[31] Channel frequency, mean length and total length characteristics appear to follow power law relationships when using least squares fitting (Figure 5). The relationship for channel frequency reveals that each channel width has approximately twice the number of channels as the next largest width, when grouped in 10 m interval bins. The total length of the narrower channels is one and a half times larger than that of the next wider channel interval. Wider channels are generally longer than narrower channels, however, there is more scatter associated with these data. These relationships may be similar to the classic scaling relationships that have been described for both river and tidal creek networks, but not as far, as we know, for floodplain channels. These scaling relationships, show patterns of structure that are self-similar or fractal-like over many orders of magnitude [Stolum, 1998; Cleveringa and Oost, 1999;

Brown et al., 2002; Rinaldo et al., 2006]. However good a power law fit, Stumpf and Porter [2012] warn against implying that this is linked to some underlying universality without both statistical support and generative mechanisms. Testing these power law fits with the approach of Clausen et al. [2009] shows that they do not cover a wide enough range in width to span more than two orders of magnitude and that theoretically other equally valid functions may also fit the data, so one needs to be careful with the interpretation. Nevertheless, Stumpf and Porter [2012] do point out that power laws have an interesting and possibly important role to play in science, and here we propose that the power law is a useful description of these data, but any conclusions regarding scaling behavior probably require more data and further analysis.

[32] While some areas of the floodplain with local runoff input exhibit similar network patterns to classic river networks, other floodplain areas that are more closely connected to the annual flooding and draining cycle and may have more similarity to tidal creek networks which are subject to twice daily flood and ebb cycles [Hibma et al., 2004]. Marsh tidal networks are strongly influenced by vegetation which stabilizes channel banks, controlling channel shape and migration [Fagherazzi et al., 1999]. Also tidal networks, unlike rivers exhibit a greater diversity in their geometrical shape and topological forms stemming from the pronounced spatial gradients of landscape-forming flow rates and competing dynamic processes [Rinaldo et al., 1999].

[33] Channel widths measured during the field survey were compared to estimates derived from the Landsat mosaic. The comparison covered 25 separate channel reaches and 101 width measurements. The difference in channel width between the two methods varies between -52 m to 54 m with a mean of 8 m, RMSE of 21.4 m and Pearson's correlation of 0.979 ($p < 0.05$) (Figure 6). The RMSE is essentially similar to, or even smaller than, the original discriminative ground resolution of the ETM+ instrument which imaged the channels (30 m), as pan sharpening to 15 m is only done after image acquisition. The comparison shows that as the channels get wider the laser range finder measurements are marginally greater than the Landsat estimate. This could be due to the following: (1) a reduction in laser range finder accuracy occurred with increased distance, (2) range finder measurements were carried out at high water and the Landsat mosaic used was at flood recession or low-water conditions when wider channels would have more bank exposed than smaller channels, or (3) the Landsat discriminative ground resolution constraint may mean that a coarse-resolution results in a blurring of channel edges. For smaller channels, laser measurements were noticeably affected by overhanging vegetation, which could alter a width measurement by as much as 10 m. Overhanging vegetation also affects the Landsat estimate. A more automated process such as that of Pavelsky and Smith [2008] for extracting the channel width may provide more detail on the widths than the method used here, although the complexity of the networks will probably still require some manual intervention.

[34] SRTM topography data are currently the only available terrain information for the Amazon floodplain and many studies of the floodplain use these data, including recent large-scale hydraulic models [Wilson et al., 2007].

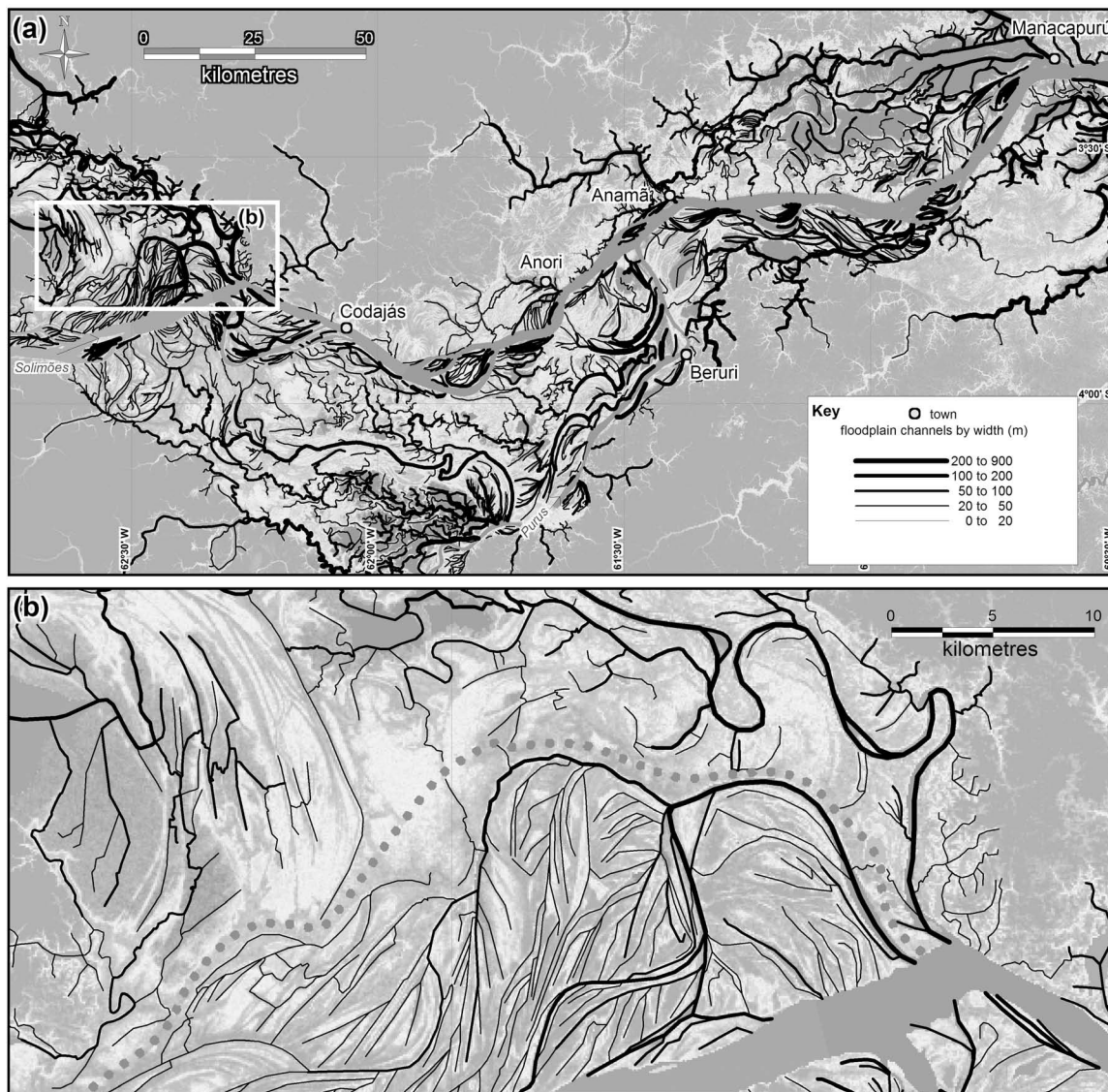


Figure 4. (a) Floodplain channels digitized from the Landsat ETM+ mosaic, shown with line thickness relative to channel width. (b) Inset showing more detail, with thick dotted line where there is very little channel connectivity.

Comparison of the floodplain channel networks derived from the Landsat mosaic with the ~ 90 m spatial resolution SRTM data of the floodplain shows that most of these floodplain channels are poorly represented in the SRTM DEM. Only around 4% of the floodplain channels have widths that are greater than the ~ 90 m SRTM resolution and some of these may also be poorly represented if they have a diagonal orientation relative to the gridded SRTM data. While these few larger channels may carry proportionally more flow than the smaller channels, most of them connect to a branching network of the smaller channels to drain the floodplain. This lack of floodplain channel representation in the SRTM topography has significant implications for any floodplain study that utilizes SRTM data to model the floodplain hydrodynamics, as it implies that significant hydraulic flow connectivity will be missing in the model. This missing flow connectivity is likely to explain some of the floodplain filling and draining problems

reported by *Wilson et al.* [2007]. The power law relationships identified here may also prove valuable in providing parameters for a simpler subgrid representation of the detailed floodplain networks at a larger scale, such as regional-scale hydrological models which are now reaching the level of resolution where the floodplain processes need to be included explicitly [*Coe et al.*, 2008; *Beighley et al.*, 2009; *Paiva et al.*, 2011].

3.2. Floodplain Channel Depth Characteristics

[35] In all, 1400 km of single line sonar survey was undertaken, and a total of 93,083 unique depth measurements were recorded, together with GPS locations for each point. Just over half (56%) of the survey specifically covered 33 floodplain channels, accessible by small boat at high water, ranging in width from 40 to 900 m and the location and extent of these are shown in Figure 7a. The floodplain channel sonar data were used for the majority of the

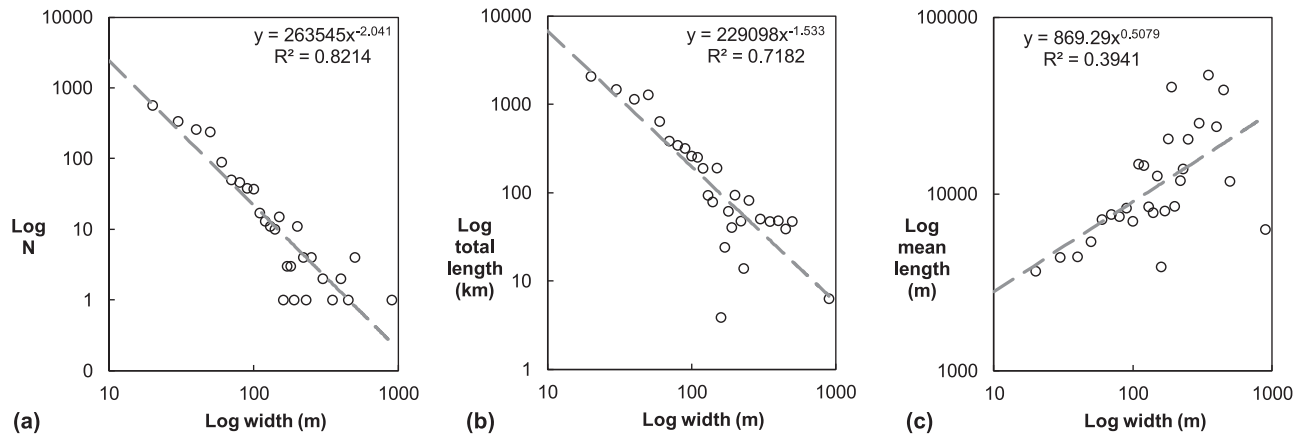


Figure 5. Log-log plots of channel characteristics with power law fits: (a) frequency versus channel width, (b) total channel length versus width, and (c) mean channel length versus width. Data are shown as open circles, and power law fit is a dashed gray line.

analysis presented here. Data from the whole survey, which included the main river channel, were used for the error analysis. Survey data were matched to the Landsat derived reaches and mean depths calculated.

[36] While the method of collecting bathymetric data using small sonar GPS units, more commonly used for fish finding, is not novel [Kvernevik *et al.*, 2002; Barbosa *et al.*, 2006; Wilson *et al.*, 2007; Trigg *et al.*, 2009], published estimates of the error associated with the method are hard to find. For this survey, an estimate of the measurement error was possible due to the many crossing tracks available from the traverses up and down channels and multiple surveys from the three bases. Unique coincident pairs of points that were located within 1 m (GPS resolution) of each other and with at least a 1 h separation in sample time were identified, resulting in 117 unique pairs of points from the full data set of 93,083 sonar depth points. Error analysis of the absolute depth difference for each pair was carried out. The mean absolute difference in depths was 0.32 m with a maximum of 1.7 m and an overall RMS difference of 0.46 m. This noise error analysis provides a

good estimate of the overall error in the survey methodology, as it includes the error associated with different river conditions, boat speeds, GPS positional accuracy as well as sonar performance and calibration. An additional source of error in the depth measurements is the change associated with the passage of the main flood wave. During the nine days of field measurements, water levels increased by 0.25 m at the Itapeuá gauging station near the upstream end of the study reach and by 0.41 m at Manacapuru gauging station near the downstream end of the study reach. These water level changes reflect the spatial and temporal uncertainty in the depths measured related to the passage of the flood wave in the main river channel.

[37] The number of channel cross sections sampled in the survey was limited due to the primary need to cover a significant line length of channels within the available time. However, the 43 cross sections that were surveyed do allow an assessment of the reliability of the estimated mean channel depth from single line sonar. Descriptive statistical analysis reveals that the overall mean standard deviation in depth for the 43 sections is 2.59 m which equates to 20% of the mean depth for all cross sections. The 23 cross sections from the channels without runoff show a generally flat bed profile with a standard deviation for the mean depth of 1.83 m (17.6% of mean depth). The 20 cross sections from the channels with local runoff show a more varied depth profile with clearly defined thalweg and have a standard deviation for the mean depth of 3.46 m (21.8% of mean depth). Two contrasting example cross sections are shown in Figure 8 emphasizing the more incised nature of the channels with runoff and the flatter profile of the channels without runoff inputs. Although in theory it is possible to derive channel slopes from the survey readings, in practice the single line sonar approach and associated error make it difficult to derive reliable estimates.

[38] Depths were found to vary consistently by channel type based on water source (Figure 9). Depths of floodplain channels with no local runoff input are clustered around a mean of 10.4 m (mean width 116 m), which is close to the mean annual vertical range of the Amazon flood wave in the study area of 10.0 m (Manacapuru, 1971–2007). A Wilcoxon rank sum test of the floodplain channel depths and

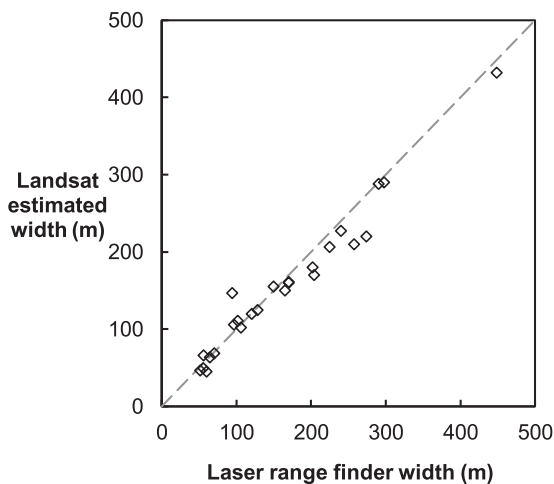


Figure 6. Channel width plot comparing laser range finder measurements with Landsat estimates.

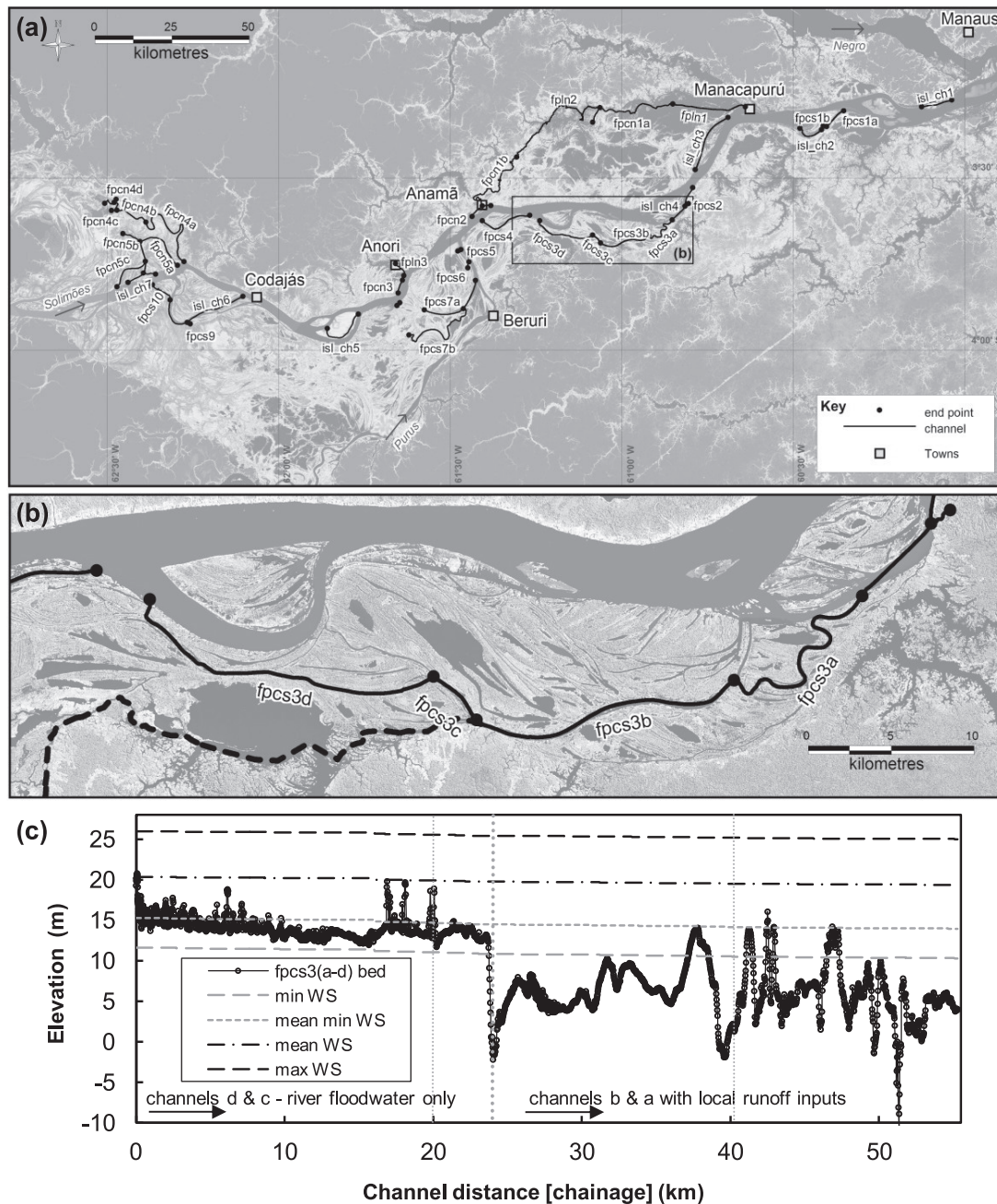


Figure 7. (a) Floodplain channel survey routes and town bases, (b) enlargement showing detail of channels fpcs3a–fpcs3d, and (c) longitudinal plot of sonar survey data with main river water level statistics: minimum, mean minimum, mean, and maximum water surface. Figures 7b and 7c show four separate, but connected, channel reaches; the first two channels (fpcs3d and fpcs3c) connect the main river to a collector channel at high water only and thus carry only river floodwater. The second two reaches (fpcs3b and fpcs3a) belong to one of the larger and deeper collector channels that run along the edge of the floodplain, with the dotted line showing the rest of this channel that connects all the way from the Purus River to the east.

the annual main channel water range time series gives a p value of 0.749 (significance level <0.05), which indicates a 75% chance the medians of these two data sets are not different. A two sample Kolmogorov-Smirnov test of the entire distribution rather than just the median gives a p value of 0.589 (significance level <0.05). This implies that the channels are formed, and their base level and slope

limited by the hydraulic head available to drain water from the floodplain back into the main channel. These drainage channels range from 50 m to 269 m in width. Channels with a local runoff input have a significantly deeper mean depth at 15.9 m (mean width 185 m), possibly due to the flows being sustained by the local catchment even when the flood flow contribution from the main river channel is

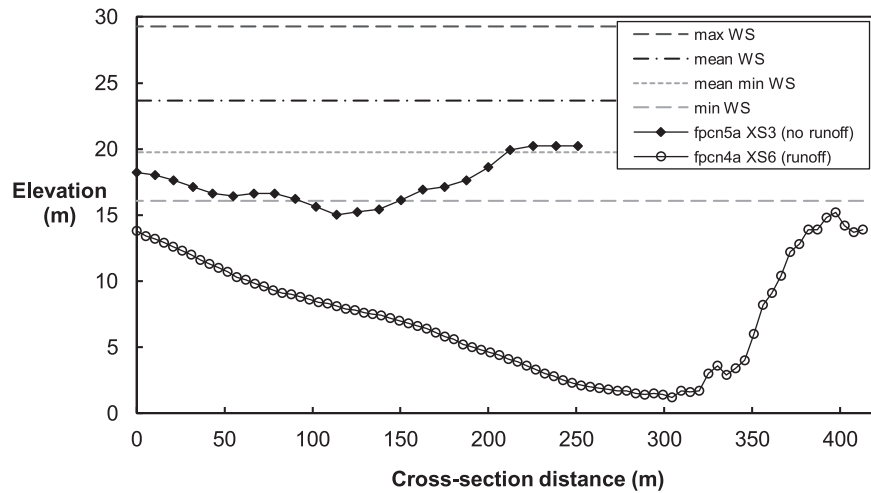


Figure 8. Contrasting example cross sections from two channels, one with local runoff showing more incised characteristics and one without local runoff, which has a flatter profile.

small. Channels strongly connected (in hydraulic terms) to the main river, and therefore exposed to the more dynamic flow regime in the main channel, tend to be much wider (mean width 520 m) and are deeper still with a mean depth of 17.7 m.

[39] We used a Wilcoxon rank sum test to interrogate whether the different samples of width and depth of the different channel types have unequal distributions. The test results revealed that all samples are significantly different from each other at the 5% significance level (p values range between 0.00011 and 0.021). The only exception was for depth when comparing the “main river channels” with “local hydrology” floodplain channels where the test showed a p value of 0.202, which means that there is a 20% chance that these two channel types may not be different in terms of depth, although they are significantly different in width ($p = 0.010$).

[40] Rowland *et al.* [2009] also found a link between the depth of floodplain tie channels, connecting the main river

to floodplain lakes, and the mean range of stage in the main channel. Rowland *et al.* [2009] hypothesized that the lower the main river channel stage the lower the draining floodplain channel can cut, before backwater effects from the main channel take effect and reduce flow velocities in the floodplain channel. Rowland *et al.* [2009] also highlight the importance of flow reversals in maintaining floodplain tie channels through the alternating mechanisms of sediment deposition during main river flow into the floodplain and subsequent bank failures during the reverse draining of the floodplain. The deeper floodplain channels measured in our survey tend to be confined to the edge of the floodplain and all “collect” local hydrology inputs from the edge of the floodplain. These collector channels are connected at the upstream and downstream end to the main river and are known to carry sediment far into the floodplain, much like the tie channels described by Rowland *et al.* [2009], and also experience flow reversals [Mertes *et al.*, 1995], but additionally have minor tributary inputs. It may be that the

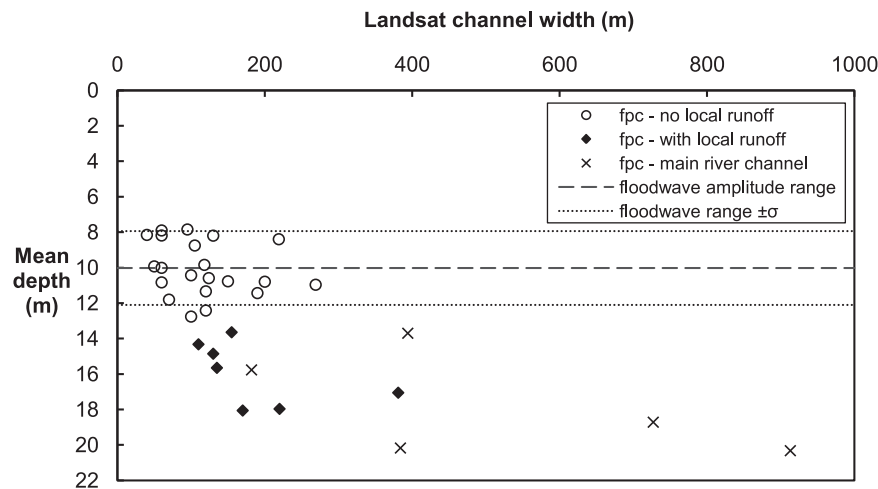


Figure 9. Mean channel depth against Landsat channel width grouped by floodplain channel (fpc) type. Note that the y axis is inverted to show depth downward. Dotted lines show the mean annual water level range (flood wave amplitude) in the adjacent Amazon River main channel and $\pm\sigma$.

extra flow input from their own local catchments, which precedes the main flood wave by a month or two, allows a stronger flow reversal and also results in higher erosive velocities even when main river channel levels are low and other floodplain channels have completed draining the previous year's river floodwater.

[41] By way of illustration, Figures 7b and 7c shows the single line sonar readings for 4 separate, but connected, channel reaches from part of the survey. The first two channels (fpcs3d and fpcs3c) connect the main river to a collector channel at high water only and thus carry only river floodwater. The second two reaches (fpcs3b and fpcs3a) belong to one of the larger and deeper collector channels, used for navigation all year round by the local population, that run along the edge of the floodplain. The dotted line shows the rest of this collector channel that connects all the way from the Purus River to the East. The depth variation in the collector channel, particularly for fpcs3a, may be the result of the channel bend morphology being picked up by the survey on this more sinuous channel, or may indicate the presence of bank slumping, but it is difficult to be sure with single line sonar data.

[42] The depth characteristics of the different channel types have important implications for studies of water transfer into, and drainage from, the floodplain: (1) Where depths are not available, it can be assumed that general floodplain channel depths can be tied to the local mean annual range of the Amazon flood wave. (2) Channels with local runoff inputs are significantly deeper than the general floodplain channels and will therefore provide preferential hydraulic flow paths throughout the flood cycle and important migration routes for aquatic species.

3.3. Floodplain Channel Networks

[43] In addition to an overall assessment of the floodplain channel characteristics, a detailed inspection of the channel network groups identified during channel digitization was undertaken. This showed that most of the network groups had very little in the way of obvious channel connections to other channel networks. Signs of possible connections between networks were observed at the upstream end of some networks but were dry in the Landsat mosaic, implying connection only at high water. Figure 10a shows the resulting 66 separate networks identified by this analysis.

[44] The existence of distinct connectivity networks as well as differences between the channel and network characteristics imply that there are different hydrological and hydraulic processes at work in these distinct areas [Western *et al.*, 2001; Michaelides and Chappell, 2009]. We grouped these networks areas into three classes based on differing hydrological input source as well as their connectivity to those inputs, the importance of which was first identified by Mertes [1997]. The three classes recognized are (1) runoff, (2) river, and (3) central. The primary distinction between classes was the presence (runoff) or absence (river and central) of local runoff inputs from terrace slopes outside the floodplain boundary. The secondary distinction between river and central classes arises from their connectivity to the main river channel. The river class networks are strongly connected to the main river channel by floodplain channels at both the upstream and downstream ends of the floodplain area, implying significant input and

drainage of river water through the floodplain channels. The central class networks are only connected to the main river through drainage channels at the downstream end of the area and any input from the main river or other floodplain areas is through predominantly diffusive overbank flow rather than channel flow.

[45] Assessment of the connectivity of the floodplain units with the main river channel in more detail allows each of the three classes of floodplain unit to be broken down into two further subclasses or types of unit. The runoff class has a direct type, which drains runoff areas external to the floodplain directly into the main channel without passing through the floodplain, and an indirect type which drains runoff areas via a collector channel through the floodplain until reaching the main river channel. The collector channel is confined to the edge of the floodplain by sediment deposits. The river class has an island type which is surrounded by the main channel on all sides and a bypass type which lie adjacent to the main channel and therefore only connect on one side of the unit. The central class has a basin type which is only connected to the main channel by its main drainage channel at the downstream end and is surrounded by other floodplain unit types, thus receives river flow inputs indirectly. The second type under the central class is the connect type which has the same properties of being surrounded by other units as the basin type except for an upstream end that lies adjacent to the main river and receives diffusive flows directly from the river at high-flood stages. Table 1 provides a summary of the classification method for the floodplain unit classes and types.

[46] These floodplain areas are here termed "floodplain hydrologic units" (FHU) as we think they represent distinct and separate areas of floodplain thought to function as single units from a hydrological perspective. While it is not suggested that these units are totally isolated from each other, it is thought that the hydrological input source, the connectivity of the networks and sediment barriers between the units ensures relative isolation of surface flows for considerable portions of the flood cycle. The units are expected to become connected at high water through diffuse flow across the boundaries between them, and are likely to be connected most of the time through groundwater flow.

[47] Other than the existence of distinct connectivity networks implying that there are different hydrological and hydraulic processes at work in these distinct areas, what other evidence is there of spatially differentiated floodplain processes related to our defined FHUs? Field measurements of floodplain channel depth presented earlier demonstrate significant differences in channel depth between areas of the floodplain that are connected to local runoff (only present in the runoff class) and those carrying only river floodwater. Mertes *et al.* [1995] also demonstrated different vegetation distributions across floodplain areas as a result of the different sources of water present and habitat types available. Latrubesse and Franzinelli [2002] mapped different sediment ages and deposition rates across the middle reach floodplain which match directly our FHU classes. Their older scroll-dominated plain areas match our indirect type of the runoff FHU class, their impeded floodplain units match our basin and connect type of the central FHU class, and finally their channel-dominated floodplain units match our bypass and island type of the river FHU class. This

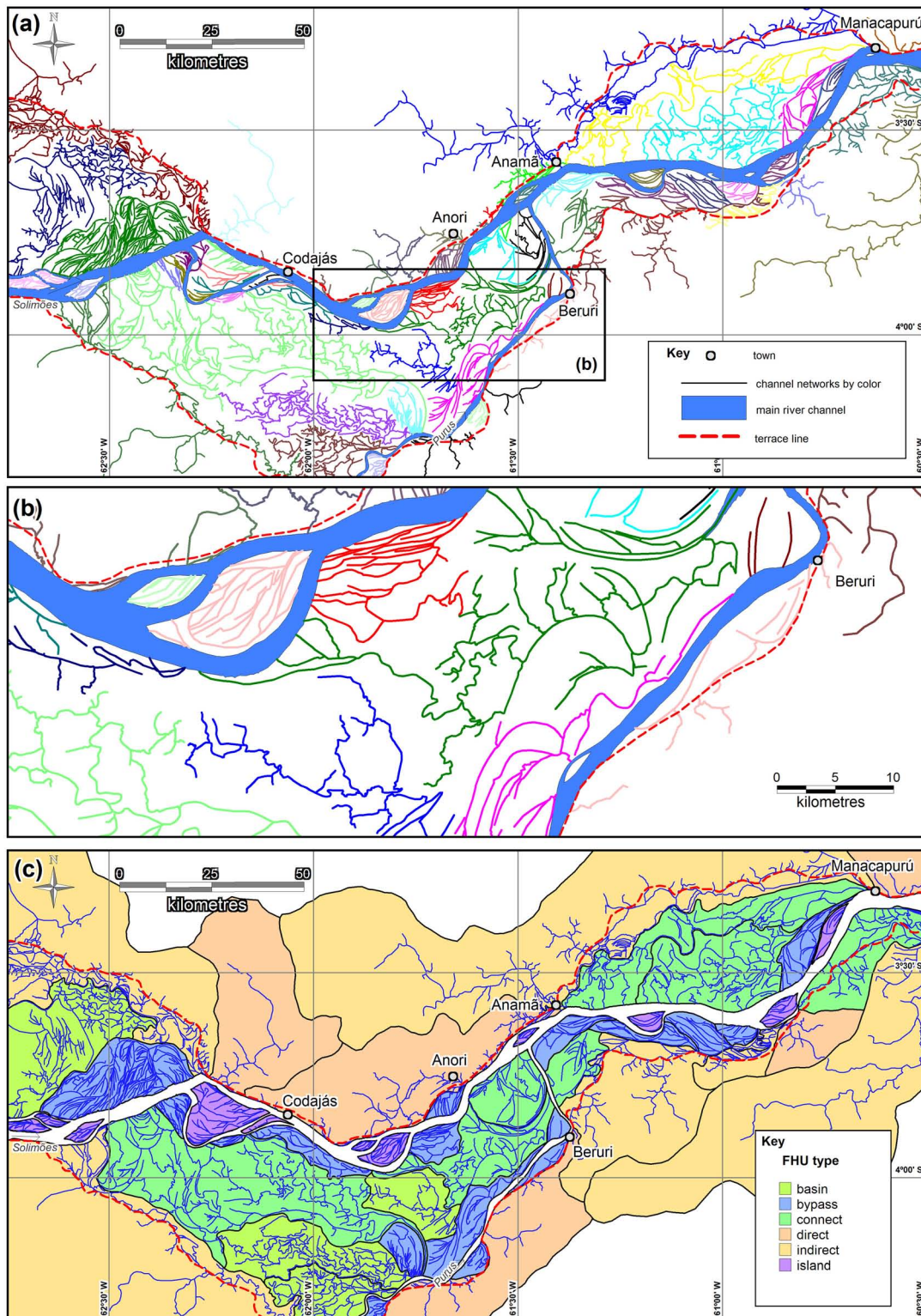


Figure 10. (a) Digitized floodplain channels colored by networks isolated from each other except at high water. (b) Detailed enlargement. (c) Floodplain hydrologic units (FHUs).

similarity in derived areas using very different analyses; i.e., connectivity versus sediment mapping provides further evidence of the underlying hydrological functional nature of the floodplain areas. *Lesack and Melack* [1995] used chemical and hydrologic data to show that the spatial extent and

volume of river water incursion into Amazon lakes depends on the ratio of the local drainage basin area to lake area and distance from the river, demonstrating again that connections to water source are important in controlling the resultant dynamics in the floodplain. Finally, measurements of

Table 1. Floodplain Hydrologic Unit Class and Type Classification

Class	Type	Main Input Water Source	Input via Channels	Main River Connection Type
Runoff	direct	runoff	yes	direct
	indirect	runoff and main river	yes	via floodplain
River	island	main river	yes	all sides
	bypass	main river	yes	One side
Central	connect	main river	no	diffusive upstream
	basin	main river	no	diffusive via other units

water level changes across the floodplain using spaceborne interferometric SAR JERS-1 by *Alsdorf et al.* [2007], during the rising water stage, demonstrate patterns of $\delta h/\delta t$ across the floodplain that are complex and regionalized and can be correlated with the floodplain channel networks. High-water patterns of $\delta h/\delta t$ are much more homogeneous, suggesting connection of these separate floodplain areas by diffuse overland flow during this period.

[48] Delineation of the areas represented by each FHU network allows the physical characteristics of these areas to be further quantified and compared, namely, frequency, area, drainage density, sinuosity, mean channel width and depth. The floodplain hydrologic units defined for the study area are shown in Figure 10c and the derived area characteristics detailed in Table 2. These physical characteristics show that river class units (island and bypass), are more numerous and smaller than the other types due to the more active sediment deposition and erosion processes occurring in these units. The mean area of indirect FHU types is by far the largest, mainly due to the fact that each collecting channel, of which there is only one in each unit, runs along the edge of large areas of floodplain picking up runoff from numerous small terrace catchments. Drainage density also varies between the FHU classes. The units of the river class have 2 times the drainage density of the central floodplain class, which in turn have 3.5 times the drainage density of the runoff class.

[49] Landsat imagery has been used previously to study the Amazon floodplain [*Puhakka et al.*, 1992; *Mertes et al.*, 1995; *Toivonen et al.*, 2007], but none of these studies have looked specifically at mapping the floodplain channels in detail and identifying networks by connectivity. *Smith and Alsdorf* [1998] used SAR amplitude data and interferometric images of the Ob River, Siberia to map multitemporal river and floodplain connectivity, identifying seasonally regulated networks important to the floodplain water and sediment exchange with the main river channels. *Pavelsky and Smith* [2009] used SPOT and ASTER images

of the Peace-Athabasca delta to map suspended sediment concentrations, revealing strong variations in water sources and flow patterns, including flow reversals in major distributaries. *Hamilton and Lewis* [1990] used Landsat images to study the physical characteristics of the fringed floodplain of the Orinoco River in Venezuela and divided the floodplain into seven reaches for interpretation and also noted that the floodplain could be grouped into spatially discrete units. However, *Hamilton and Lewis's* [1990] units were used to refer to large areas of floodplain on both sides of the river and not to divisions within the floodplain, and are therefore different to the FHUs described here. Instead, the FHUs defined here can be thought of hydrogeomorphic units, a term used to refer to a land form characterized by a specific origin, geomorphic setting, water source, and hydrodynamics [e.g., *Cole et al.*, 2002; *Nardi et al.*, 2006].

[50] While other research has shown that there are distinct areas of the floodplain with different properties, particularly *Mertes et al.* [1995] and *Latrubesse and Franzinelli* [2002], this is the first attempt to provide a consistent methodology for breaking down the complex heterogeneity of the Amazon floodplain into functional units based on hydrological connectivity and functionality. Evidence that these units do function as separate units has been presented through field measurements, network connectivity and area analysis as well as through reference to other published work. Further research data are required to test the FHU hypothesis and demonstrate the functional detail of the FHU units and it is hoped that emerging methodologies (see *Hall et al.* [2011] for a review) for mapping water elevations [*Durand et al.*, 2010; *Hall et al.*, 2012] and changes in water level [*Alsdorf et al.*, 2007] from space will provide the tools for further testing and development of this proposed hydrodynamic framework, as well as providing valuable new insights into this complex dynamic natural system and the evolution of floodplain units.

[51] The fact that the defined FHUs have very different hydrological characteristics (e.g., drainage density and

Table 2. Characteristics of Floodplain Hydrologic Units

Class	FHU Type	Count	Area (km ²)	Percentage of Total Area	Mean Area (km ²)	Total Channel Length (km)	Drainage Density (km/km ²)	Channel Mean Sinuosity	Channel Mean Width (m)	Mean Surveyed Channel Depth ^a (m)
Runoff	indirect	6	12,082	48.2%	2010	2214	0.32	1.17	57.8	15.9 (7)
	direct	5	4037	16.1%	807	573	0.24	1.14	38.0	— (0)
River	island	11	501	2.0%	46	579	1.99	1.04	63.9	15.3 (7)
	bypass	17	1918	7.7%	113	2098	1.88	1.07	40.6	9.8 (11)
Central	connect	7	4492	17.9%	642	2500	0.96	1.20	44.1	10.3 (6)
	basin	4	2019	8.1%	505	1329	1.13	1.24	41.4	11.6 (2)
Overall		50	25,050		501	9293	0.64	1.15	46.9	12.5 (33)

^aSample size is given in parentheses.

water sources) has important implications for many biogeochemical studies in the Amazon which rely on an understanding of these characteristics in order to quantify and estimate dependent processes. The relative distribution of nutrient rich river flood water versus local sources of water for the várzea, the interface of which was defined as the perirheic zone by Mertes [1997], is important in analyzing the nutrient cycling and hence biomass production of the region [Junk and Piedade, 1993; Melack and Forsberg, 2001]. This floodplain productivity also has important implications for the calculation of global carbon fluxes [Grace and Malhi, 2002].

[52] Knowledge of a floodplain area's connectivity to other areas and the main channel is also important in terms of assessing environmental impacts of potential spills from oil pipelines and therefore the planning of mitigation strategies such as avoiding well connected areas and the deeper floodplain channels. Finally, the existence of floodplain functional units can be used to test how good recent attempts at large-scale hydrodynamic modeling are at capturing the detailed hydrodynamics of the Amazon River and floodplain [Wilson et al., 2007], especially given the lack of the representation of floodplain channel networks in the SRTM data. It may also provide a basis for detailed sediment transport and source-pathway-receptor studies.

4. Conclusions

[53] Amazonian floodplain channels are relatively understudied and the research presented in this paper represents the first dedicated and rigorous study of the morphological characteristics of a large number of these floodplain channels from a transitional reach of the middle Amazon River using a combination of remote sensing image analysis and field survey.

[54] Previous research has identified floodplain channels as an important component of the Amazon floodplain, but has relied largely on qualitative descriptive evidence for an understanding of their properties and function. We quantify some of these unknown floodplain channel characteristics and show they that not only are floodplain channels important to many physical and biological processes in the floodplain, but that they are ubiquitous and organized into functionally distinct networks controlled by physical processes related to terrain and water source.

[55] Our analysis shows that floodplain channels are numerous and cover a range of widths from 10–1000 m with a mean width of 47 m, and confirms that they play an important role in the dynamic exchange of water between the main river channel and floodplain as well as from surrounding hillslopes to the main channel. We show that some floodplain channel characteristics can usefully be described using power laws which may indicate self-similar or fractal like behavior, much like has been hypothesized for other types of fluvial networks such as rivers drainage systems. Comparison of the floodplain channel widths with the SRTM terrain data of the floodplain shows that only a small fraction of the channels (~4%) are wider than the ~90 m spatial resolution topography of SRTM. This has significant implications for any studies of the hydrodynamics of the floodplain using SRTM data.

[56] Mean channel depths were found to vary consistently when grouped by channel type. The mean depth of flood-

plain channels with no runoff input (10.4 m) appears to be related to the mean annual vertical range of the Amazon flood wave (10 m, ± 2 m σ), which is the main driver for the filling and draining of these channels. Channels with a local runoff input have a significantly deeper mean depth (15.9 m) due to the flows being sustained by the local catchment even when the flood flow contribution from the main river channel is small. Channels considered as minor branches of the main channel tend, unsurprisingly, to be much wider (mean width 520 m) than other floodplain channels and are deeper (17.7 m). These depth characteristics have important implications for studies related to water transfer between river and floodplain and can be used where no floodplain channel depth measurements are readily available. In addition, the deeper floodplain channels with local runoff inputs and main river branch channels will provide preferential hydraulic flow paths for filling and draining of the floodplain and may also be important migration routes for aquatic species.

[57] Despite the inherent complexity of the floodplain channel networks, our analysis shows that there are distinct and mostly separate networks of channels in the floodplain that can be grouped by their physical characteristics, representing distinct separate areas of floodplain that seem to function as single units from a hydrological perspective, here termed floodplain hydrologic units. This is the first time that breaking down the complex heterogeneity of the Amazon floodplain into hydrological functional units has been explored. While further work is required to extend this concept across the wider Amazon floodplain, this initial approach can form a solid basis for a more detailed, systematic framework for understanding the hydrodynamics of the Amazon River and floodplain.

[58] **Acknowledgments.** The research reported in this paper was undertaken as part of a PhD in the School of Geographical Sciences, University of Bristol, and was supported by the Natural Environment Research Council (grant NER/S/A/2006/14062). The final paper was completed under funding provided by the Willis Research Network. We thank our Amazon guide and all-around adventurer Clive Maguire for the use of his boat and services, which proved invaluable for the data collection and fieldwork in remote locations on the Amazon floodplain. Part of Guy Schumann's time was funded by a Great Western Research fellowship. Special thanks are also extended to the reviewers, who provided useful and constructive criticism of the initial drafts of this paper.

References

- Alsdorf, D. E. (2003), Water storage of the central Amazon floodplain measured with GIS and remote sensing imagery, *Ann. Assoc. Am. Geogr.*, 93(1), 55–66.
- Alsdorf, D., T. Dunne, J. Melack, L. Smith, and L. Hess (2005), Diffusion modeling of recession flow on central Amazonian floodplains, *Geophys. Res. Lett.*, 32, L21405, doi:10.1029/2005GL024412.
- Alsdorf, D., P. Bates, J. Melack, M. Wilson, and T. Dunne (2007), Spatial and temporal complexity of the Amazon flood measured from space, *Geophys. Res. Lett.*, 34, L08402, doi:10.1029/2007GL029447.
- Barbosa, C. C. F., E. M. Leão de Moraes Novo, J. M. Melack, R. Morais de Freitas, and W. P. Filho (2006), A methodology for analysis of volume and flooded area dynamics: Lago Grande de Curuai várzea as an example, *Braz. J. Cartogr.*, 58(3), 201–210.
- Barroux, G., J. E. Sonke, G. Boaventura, J. Viers, Y. Godderis, M. P. Bonnet, F. Sondag, S. Gardoll, C. Lagane, and P. Seyler (2006), Seasonal dissolved rare earth element dynamics of the Amazon River main stem, its tributaries, and the Curuai floodplain, *Geochim. Geophys. Geosyst.*, 7, Q12005, doi:10.1029/2006GC001244.
- Beighley, R. E., K. G. Eggert, T. Dunne, Y. He, V. Gummadi, and K. L. Verdin (2009), Simulating hydrologic and hydraulic processes throughout the Amazon River Basin, *Hydrol. Processes*, 23(8), 1221–1235.

- Bonnet, M. P., G. Barroux, P. Seyler, G. Pecly, P. Moreira-Turcq, C. Lagane, G. Cochonneau, J. Viers, F. Seyler, and J. L. Guyot (2005), Seasonal-links between the Amazon-corridor and its flood plain: The case of the varzea of Curuai, paper presented at International Symposium on Dynamics and Biogeochemistry of River Corridors and Wetlands held at the 7th Scientific Assembly of the International Association of Hydrological Sciences, Foz do Iguaçu, Brazil, 3–9 April.
- Bonnet, M. P., et al. (2008), Floodplain hydrology in an Amazon floodplain lake (Lago Grande de Curuai), *J. Hydrol.*, **349**, 18–30.
- Brown, J. H., V. K. Gupta, B. L. Li, B. T. Milne, C. Restrepo, and G. B. West (2002), The fractal nature of nature: Power laws, ecological complexity and biodiversity, *Philos. Trans. R. Soc. B*, **357**(1421), 619–626.
- Clauset, A., C. R. Shalizi, and M. E. J. Newman (2009), Power-law distributions in empirical data, *SIAM Rev.*, **51**(4), 661–703.
- Cleveringa, J., and A. P. Oost (1999), The fractal geometry of tidal-channel systems in the Dutch Wadden Sea, *Geol. Mijnb.*, **78**(1), 21–30.
- Coe, M. T., M. H. Costa, and E. A. Howard (2008), Simulating the surface waters of the Amazon River basin: Impacts of new river geomorphic and flow parameterizations, *Hydrol. Processes*, **22**(14), 2542–2553.
- Cole, C. A., R. P. Brooks, P. W. Shaffer, and M. E. Kentula (2002), Comparison of hydrology of wetlands in Pennsylvania and Oregon (USA) as an indicator of transferability of hydrogeomorphic (HGM) functional models between regions, *Environ. Manage.*, **30**(2), 265–278.
- Day, G., W. E. Dietrich, J. C. Rowland, and A. Marshall (2008), The depositional web on the floodplain of the Fly River, Papua New Guinea, *J. Geophys. Res.*, **113**, F01S02, doi:10.1029/2006JF000622.
- Dillabaugh, C. R., K. O. Niemann, and D. E. Richardson (2002), Semi-automated extraction of rivers from digital imagery, *Geoinformatica*, **6**(3), 263–284.
- Dunne, T., L. A. K. Mertes, R. H. Meade, J. E. Richey, and B. R. Forsberg (1998), Exchanges of sediment between the flood plain and channel of the Amazon River in Brazil, *Geol. Soc. Am. Bull.*, **110**(4), 450–467.
- Durand, M., E. Rodriguez, D. E. Alsdorf, and M. Trigg (2010), Estimating river depth from remote sensing swath interferometry measurements of river height, slope, and width, *IEEE J. Sel. Top. Appl. Earth Obs. Remote Sens.*, **3**(1), 20–31.
- Engle, D., and J. M. Melack (2000), Methane emissions from an Amazon floodplain lake: Enhanced release during episodic mixing and during falling water, *Biogeochemistry*, **51**(1), 71–90.
- Fagherazzi, S., A. Bortoluzzi, W. E. Dietrich, A. Adami, S. Lanzoni, M. Marani, and A. Rinaldo (1999), Tidal networks: 1. Automatic network extraction and preliminary scaling features from digital terrain maps, *Water Resour. Res.*, **35**(12), 3891–3904.
- Forsberg, B. R., Y. Hashimoto, A. Rosenqvist, and F. P. de Miranda (2000), Tectonic fault control of wetland distributions in the central Amazon revealed by JERS-1 radar imagery, *Quaternary Int.*, **72**(1), 61–66, doi:10.1016/S1040-6182(00)00021-5.
- Grace, J., and Y. Malhi (2002), Global change: Carbon dioxide goes with the flow, *Nature*, **416**(6881), 594–595.
- Hall, A. C., G. J. P. Schumann, J. L. Bamber, and P. D. Bates (2011), Tracking water level changes of the Amazon Basin with space-borne remote sensing and integration with large scale hydrodynamic modelling: A review, *Phys. Chem. Earth*, **36**(7–8), 223–231.
- Hall, A. C., G. J.-P. Schumann, J. L. Bamber, P. D. Bates, and M. A. Trigg (2012), Geodetic corrections to gauges on large rivers using ICESat altimetry, *Water Resour. Res.*, **48**, W06602, doi:10.1029/2011WR010895.
- Hamilton, S. K., and W. M. Lewis (1990), Physical characteristics of the fringing floodplain of the Orinoco River, Venezuela, *Interciencia*, **15**(6), 491–500.
- Hess, L. L., J. M. Melack, E. Novo, C. C. F. Barbosa, and M. Gastil (2003), Dual-season mapping of wetland inundation and vegetation for the central Amazon basin, *Remote Sens. Environ.*, **87**(4), 404–428.
- Hibma, A., M. J. F. Stive, and Z. B. Wang (2004), Estuarine morphodynamics, *Coastal Eng.*, **51**(8–9), 765–778.
- Junk, W. J. (1993), *Wetlands of Tropical South America*, Kluwer, Dordrecht, Netherlands.
- Junk, W. J., and M. T. F. Piedade (1993), Biomass and primary-production of herbaceous plant-communities in the Amazon floodplain, *Hydrobiologia*, **263**(3), 155–162.
- Kvernevik, T. I., M. Zambri Mohd Akhir, and J. Studholme (2002), A low-cost procedure for automatic seafloor mapping, with particular reference to coral reef conservation in developing nations, *Hydrobiologia*, **474** (1–3), 67–79.
- Latrubesse, E. M., and E. Franzinelli (2002), Holocene alluvial plain of the middle Amazon River, Brazil, *Geomorphology*, **44**(3–4), 241–257, doi:10.1016/S0169-555X(01)00177-5.
- Lesack, L. F. W. (1995), Seepage exchange in an Amazon floodplain lake, *Limnol. Oceanogr.*, **40**(3), 598–609.
- Lesack, L. F. W., and J. M. Melack (1995), Flooding hydrology and mixture dynamics of lake water derived from multiple sources in an Amazon floodplain lake, *Water Resour. Res.*, **31**(2), 329–345.
- Martinez, J. M., and T. Le Toan (2007), Mapping of flood dynamics and spatial distribution of vegetation in the Amazon floodplain using multi-temporal SAR data, *Remote Sens. Environ.*, **108**(3), 209–223.
- Melack, J. M., and B. R. Forsberg (2001), Biogeochemistry of Amazon floodplain lakes and associated wetlands, in *The Biogeochemistry of the Amazon Basin and Its Role in a Changing World*, edited by M. E. McClain, R. L. Victoria, and J. E. Richey, pp. 235–276, Oxford Univ. Press, Oxford, U. K.
- Mertes, L. A. K. (1997), Documentation and significance of the perirheic zone on inundated floodplains, *Water Resour. Res.*, **33**(7), 1749–1762.
- Mertes, L. A. K., M. O. Smith, and J. B. Adams (1993), Estimating suspended sediment concentrations in surface waters of the Amazon River wetlands from Landsat images, *Remote Sens. Environ.*, **43**(3), 281–301.
- Mertes, L. A. K., D. L. Daniel, J. M. Melack, B. Nelson, L. A. Martinelli, and B. R. Forsberg (1995), Spatial patterns of hydrology, geomorphology, and vegetation on the floodplain of the Amazon River in Brazil from a remote-sensing perspective, *Geomorphology*, **13**(1–4), 215–232.
- Mertes, L. A. K., T. Dunne, and L. A. Martinelli (1996), Channel-floodplain geomorphology along the Solimoes-Amazon River, Brazil, *Geol. Soc. Am. Bull.*, **108**(9), 1089–1107.
- Michaelides, K., and A. Chappell (2009), Connectivity as a concept for characterising hydrological behaviour, *Hydrol. Processes*, **23**(3), 517–522.
- Nardi, F., E. R. Vivoni, and S. Grimaldi (2006), Investigating a floodplain scaling relation using a hydrogeomorphic delineation method, *Water Resour. Res.*, **42**, W09409, doi:10.1029/2005WR004155.
- Paiva, R. C. D., W. Collischonn, and C. E. M. Tucci (2011), Large scale hydrologic and hydrodynamic modeling using limited data and a GIS based approach, *J. Hydrol.*, **406**(3–4), 170–181.
- Panosso, R. D., D. Muehe, and F. D. Esteves (1995), Morphological characteristics of an Amazon floodplain lake (Lake Batata, Para State, Brazil), *Amazoniana Limnol. Oecol. Regionalis Syst. Fluminis Amazonas*, **13**(3–4), 245–258.
- Pavelsky, T. M., and L. C. Smith (2008), RivWidth: A software tool for the calculation of river widths from remotely sensed imagery, *IEEE Geosci. Remote Sens. Lett.*, **5**(1), 70–73.
- Pavelsky, T. M., and L. C. Smith (2009), Remote sensing of suspended sediment concentration, flow velocity, and lake recharge in the Peace-Athabasca Delta, Canada, *Water Resour. Res.*, **45**, W11417, doi:10.1029/2008WR007424.
- Peixoto, J. M. A., B. W. Nelson, and F. Wittmann (2009), Spatial and temporal dynamics of river channel migration and vegetation in central Amazonian white-water floodplains by remote-sensing techniques, *Remote Sens. Environ.*, **113**(10), 2258–2266.
- Puhakka, M., R. Kalliola, M. Rajasilta, and J. Salo (1992), River types, site evolution and successional vegetation patterns in Peruvian Amazonia, *J. Biogeogr.*, **19**(6), 651–665.
- Richey, J. E., L. A. K. Mertes, T. Dunne, R. L. Victoria, B. R. Forsberg, A. C. N. S. Tancredi, and E. Oliveira (1989), Sources and routing of the Amazon River flood wave, *Global Biogeochem. Cycles*, **3**(3), 191–204.
- Rinaldo, A., S. Fagherazzi, S. Lanzoni, M. Marani, and W. E. Dietrich (1999), Tidal networks: 2. Watershed delineation and comparative network morphology, *Water Resour. Res.*, **35**(12), 3905–3917.
- Rinaldo, A., J. R. Banavar, and A. Maritan (2006), Trees, networks, and hydrology, *Water Resour. Res.*, **42**, W06D07, doi:10.1029/2005WR004108.
- Rossetti, D. D., P. M. de Toledo, and A. M. Goes (2005), New geological framework for western Amazonia (Brazil) and implications for biogeography and evolution, *Quat. Res.*, **63**(1), 78–89.
- Rowland, J. C., W. E. Dietrich, G. Day, and G. Parker (2009), Formation and maintenance of single-thread tie channels entering floodplain lakes: Observations from three diverse river systems, *J. Geophys. Res.*, **114**, F02013, doi:10.1029/2008JF001073.
- Smith, L. C., and D. E. Alsdorf (1998), Control on sediment and organic carbon delivery to the Arctic Ocean revealed with spaceborne synthetic aperture radar: Ob' River, Siberia, *Geology*, **26**(5), 395–398.

- Stolum, H. H. (1998), Planform geometry and dynamics of meandering rivers, *Geol. Soc. Am. Bull.*, 110(11), 1485–1498.
- Stumpf, M. P. H., and M. A. Porter (2012), Critical truths about power laws, *Science*, 335(6069), 665–666.
- Toivonen, T., S. Maeki, and R. Kalliola (2007), The riverscape of western Amazonia: a quantitative approach to the fluvial biogeography of the region, *J. Biogeogr.*, 34, 1374–1387, doi:10.1111/j.1365-2699.2007.01741.x.
- Trigg, M. A., M. D. Wilson, P. D. Bates, M. S. Horritt, D. E. Alsdorf, B. R. Forsberg, and M. C. Vega (2009), Amazon flood wave hydraulics, *J. Hydrol.*, 374(1–2), 92–105.
- Western, A. W., G. Bloschl, and R. B. Grayson (2001), Toward capturing hydrologically significant connectivity in spatial patterns, *Water Resour. Res.*, 37(1), 83–97.
- Wilson, M., P. Bates, D. Alsdorf, B. Forsberg, M. Horritt, J. Melack, F. Frappart, and J. Famiglietti (2007), Modeling large-scale inundation of Amazonian seasonally flooded wetlands, *Geophys. Res. Lett.*, 34, L15404, doi:10.1029/2007GL030156.
- Wittmann, F., W. J. Junk, and M. T. F. Piedade (2004), The varzea forests in Amazonia: Flooding and the highly dynamic geomorphology interact with natural forest succession, *For. Ecol. Manage.*, 196(2–3), 199–212.